

Sulfur isotope fractionations constrain the biological cycling of dimethylsulfoniopropionate in the upper ocean

Daniela Osorio-Rodriguez¹,^{*} Manuel Razo-Mejia,² Nathan F. Dalleska,¹ Alex L. Sessions,¹ Victoria J. Orphan,¹ Jess F. Adkins^{1*}

¹Division of Geological and Planetary Sciences, California Institute of Technology, Pasadena, California

²Division of Biology and Biological Engineering, California Institute of Technology, Pasadena, California

Abstract

The rapid turnover of dimethylsulfoniopropionate (DMSP), likely the most relevant dissolved organic sulfur compound in the surface ocean, makes it pivotal to understand the cycling of organic sulfur. Dimethylsulfoniopropionate is mainly synthesized by phytoplankton, and it can be utilized as carbon and sulfur sources by marine bacteria or cleaved by bacteria or algae to produce the volatile compound dimethylsulfide (DMS), involved in the formation of sulfate aerosols. The fluxes between the consumption (i.e., demethylation) and cleavage pathways are thought to depend on community interactions and their sulfur demand. However, a quantitative assessment of the sulfur partitioning between each of these pathways is still missing. Here, we report for the first time the sulfur isotope fractionations by enzymes involved in DMSP degradation with different catalytic mechanisms, expressed heterologously in *Escherichia coli*. We show that the residual DMSP from the demethylation pathway is 2.7‰ enriched in $\delta^{34}\text{S}$ relative to the initial DMSP, and that the fractionation factor ($^{34}\epsilon$) of the cleavage pathways varies between -1 and -9 ‰. The incorporation of these fractionation factors into mass balance calculations constrains the biological fates of DMSP in seawater, supports the notion that demethylation dominates over cleavage in marine environments, and could be used as a proxy for the dominant pathways of degradation of DMSP by marine microbial communities.

Dissolved organic sulfur is comprised of 432 identified compounds (Tang 2020), and at least 800 compounds predicted by mass and structure (Ksionzek et al. 2016). Dimethylsulfoniopropionate (DMSP) is the most abundant known and quantifiable dissolved organic S species, contributing 2.3% of the minimum estimated marine dissolved organic S (Ksionzek et al. 2016) at an average concentration of 1–2 nM (Kiene and Slezak 2006; Levine et al. 2016). Dimethylsulfoniopropionate producers can accumulate it intracellularly, generating a particulate DMSP pool with concentrations up to nearly 500 mM inside the cell (Mcparland and Levine 2019). The production of DMSP is mainly attributed to marine phytoplankton (Keller 1989), although bacteria and corals are low DMSP producers (Mcparland and Levine 2019). It has a turnover of hours to days (Zubkov et al. 2002; Galí and Simó 2015; Levine et al. 2016), and has

been hypothesized to be involved in different physiological functions, including protection from cold (Kirst et al. 1991; Karsten et al. 1996), osmotic (Dickson and Kirst 1987), and oxidative stresses (Sunda et al. 2002). One of the biological degradation products of DMSP, dimethylsulfide (DMS), gathered atmospheric chemistry research attention on volatile dissolved organic S more than 30 years ago, when its potential to influence global climate by means of aerosol formation was first pointed out (Charlson et al. 1987). The so-called CLAW hypothesis predicted a negative climate feedback where Earth's temperature would be regulated by the interaction between sulfur emissions from phytoplankton and cloud formation. Although DMS emissions might actually not be significant for global climate regulation under a warming scenario (i.e., Quinn and Bates 2011), they are expected to alter the regional formation of sulfate aerosols (Sanchez et al. 2018), with potential impacts on the weather at high latitudes (Wang et al. 2018).

Beyond DMS, dissolved organic S is usually disregarded by sulfur biogeochemists because its abundance in seawater is exceeded by six orders of magnitude by that of sulfate (Ksionzek et al. 2016), which has a concentration of 28 mM (Morris and Riley 1966). The fact that sulfate is an important electron acceptor, responsible for the remineralization of up to half of the organic matter in coastal sediments

*Correspondence: dosorior@caltech.edu, jess@gps.caltech.edu

This is an open access article under the terms of the Creative Commons Attribution-NonCommercial License, which permits use, distribution and reproduction in any medium, provided the original work is properly cited and is not used for commercial purposes.

Additional Supporting Information may be found in the online version of this article.

(Jorgensen 1982), and that it leaves a fingerprint in the rock record as sulfate or sulfide (its reduction product) minerals, has made it central in the study of the geologic sulfur cycle (Garrels and Lerman 1981). Nonetheless, the slow turnover of sulfate, which has a residence time of $\sim 10^7$ years in the ocean (Holland 1973), highlights the relevance of addressing the dynamics of highly labile dissolved organic S, such as DMSP and DMS, toward a comprehensive understanding of the short-scale processes that may affect the sulfur cycle. Reduced sulfur, and in particular dissolved organic S, might also be fundamental to understanding the sulfur cycle during the Archaean, where oxygen and sulfate concentrations were negligible (Fakhraee and Katsev 2019).

Recently, microbial ecologists have rekindled interest in DMSP as the role of dissolved organic S in ecosystem dynamics has been highlighted (Levine 2016). Both DMSP and DMS have been demonstrated to be strong chemoattractants for marine bacteria and zooplankton (i.e., Seymour et al. 2010). Furthermore, DMSP induces the production of quorum sensing molecules (Johnson et al. 2016), is a mediator of bacterial virulence toward DMSP-producing algae (Barak-Gavish et al. 2018), and its cleavage to DMS may generate acrylate as a byproduct, considered to be a potential predator deterrent (i.e., Wolfe et al. 1997). Dimethylsulfoniopropionate has also been proven to satisfy up to 13% of the carbon (Levine et al. 2016), and 100% of the sulfur demand of marine heterotrophic bacteria (Kiene and Linn 2000). In fact, the most abundant marine bacteria (SAR11 clade) are not able to assimilate sulfate and rely exclusively on DMSP and other reduced sulfur compounds to satisfy their sulfur requirements (Tripp et al. 2008). Getting to know the relative routing of DMSP between the demethylation

(i.e., consumption) pathway vs. the cleavage (DMS generating) pathways (Fig. 1) is then critical to understand the importance of DMSP and DMS in the marine trophic webs, both as nutrient sources and as ecologically relevant molecules.

Insight into the relative contributions that each of the demethylation and cleavage genes/pathways may have to the fate of DMSP in seawater has been gained from studies with ^{35}S -labeled DMSP (Kiene and Linn 2000), stable sulfur isotopes, and ocean expeditions data. The Global Ocean (GOS; Rusch et al. 2007) and Tara Oceans (Pesant et al. 2015) expeditions have collected both chemical (concentrations and sulfur isotopic compositions) and biological (genomic, transcriptomic and proteomic) information relevant to the dynamics of DMSP and DMS. Sulfur isotopes are deemed the most direct and precise geochemical proxies to trace the transformations of sulfur as it moves through different reservoirs (reviewed by Fike et al. 2015). Sulfur isotope measurements of DMSP and DMS in marine surface waters (Amrani et al. 2013; Carnat et al. 2018), as well as the fractionation in the DMS produced from DMSP in marine algae (Oduro et al. 2012) were the first attempts to identify a S isotopic signature during DMSP transformations. Although these fractionation factors constitute a proxy for the eukaryotic cleavage pathway, specific $\delta^{34}\text{S}$ signatures for the demethylation pathway and the bacterial cleavage pathways have not been determined.

Here, we constrained for the first time the S isotope fractionations of individual enzymes involved in the cleavage (DMSP lyases) and demethylation (DMSP demethylase) pathways of DMSP. We performed mass balance calculations to model how the relative contributions of the different biological processes that act on DMSP account for the $\delta^{34}\text{S}$ values of

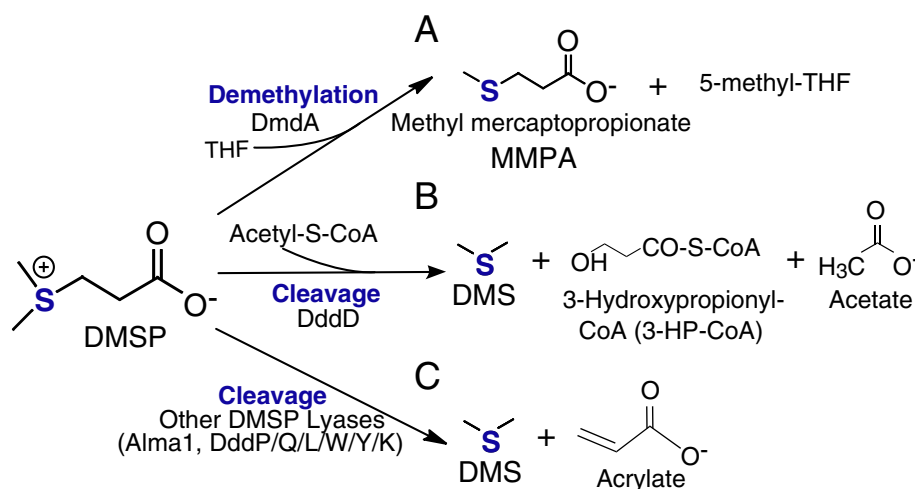


Fig 1. Biological fates of DMSP (modified from Lei et al. 2018a). **(A)** Demethylation pathway. The first step (shown here) is catalyzed by DmdA, which uses tetrahydrofolate (THF) as a cofactor (Reisch et al. 2008). This pathway is utilized for the consumption of DMSP as a carbon and sulfur source by marine bacteria. **(B)** Cleavage pathway with production of 3-Hydroxypropionyl CoA, catalyzed by DddD. This pathway requires acetyl-CoA as cofactor (Alcolombri et al. 2014b). **(C)** Cleavage pathway with production of acrylate, catalyzed by DMSP lyases other than DddD. Both **(B)** and **(C)** produce DMS, a volatile S species that is usually released to the water column.

total (particulate + dissolved) DMSP in seawater. Our data suggest that the fractionation imparted by the DMSP degrading enzymes is small, but nonetheless useful as a proxy for the main biological degradation pathways of DMSP in natural samples. Thus, the fractionation factors reported here provide a way to establish the relevance of the different cleavage pathways of DMSP in natural environments.

Methods

Cultures and extraction of cell lysates

We obtained cell lysates from *Escherichia coli* BL21 cells independently transformed with DmdA, the only DMSP demethylase described to date (kindly provided by Will Whitman from the University of Georgia, Athens), and different DMSP lyases (kindly provided by Dan Tawfik from the Weizmann Institute of Science, Israel), under control of the lac promoter. These clones were used to individually express each enzyme and had the advantage that their transcription could be regulated with the incorporation of the lac operator inducer. We do not have a reason to expect that the expression of the enzymes in *E. coli* would affect their S isotope fractionations. The clones are listed in Table 1, and the natural taxonomic distributions of each enzyme are reviewed by Lei et al. (2018a).

Each of the *E. coli* transformants was separately grown in Luria-Bertani (LB) agar plates incubated overnight at 37°C. Individual colonies retrieved from the solid media were used to inoculate 5 mL liquid LB medium for overnight incubations at 37°C, and 1 mL of these cultures was added to flasks with 1 L of sterile liquid LB media, that were kept at 37°C until they reached an OD₆₀₀ of 0.6–0.8 (late exponential phase). Solid and liquid culture media were supplemented with the corresponding antibiotic (50 µg/mL ampicillin or kanamycin), which inhibits the growth of cells that do not possess the corresponding cloning vectors. The enzyme induction and the extraction of cell lysates were performed following a modification of a previously described protocol (Lei et al. 2018b).

Briefly, the growth temperature was reduced to 16°C, and enzyme expression was induced overnight with 0.1 mM of the lac operator inducer isopropyl β-d-1-thiogalactopyranoside (IPTG). The cells were harvested by centrifugation at 4°C and resuspended in lysis buffer (5 mM Tris-HCl pH 8.0, 0.2 g/L lysozyme), followed by sonication (10 s on, 10 s off for 4 min) and subsequent centrifugation at 10,000 × g for 1 h. Total protein concentration in the crude extracts was determined using the Bio-Rad Bradford reagent with bovine serum albumin as the standard. The average concentration of each heterologous enzyme was calculated by order of magnitude approximations following So et al. (2011).

Dimethylsulfoniopropionate biodegradation experiments

Dimethylsulfoniopropionate degradation by cell lysates with each one of the enzymes in Table 1 was individually assayed in a similar way as previously described (Lei et al. 2018b). A DMSP stock solution was prepared by mixing solid DMSP (Sigma-Aldrich) with reaction buffer (5 mM Tris-HCl pH 8.0), utilized to provide a suitable pH buffering for the enzymatic reactions. Reaction assays were set up in triplicates by mixing crude cell extracts, DMSP stock, and reaction buffer in plastic vials with a total volume between 1 and 5 mL at 28°C. The cell lysates were added at an estimated total protein concentration of 5.6 mg/mL for DmdA, 1 µg/mL for Alma1, 8.2 mg/mL for DddP, 14 µg/mL for DddY, 0.9 mg/mL for DddK, 3 mg/mL for DddQ, and 0.6 mg/mL for DddD, which allowed to observe DMSP degradation over similar periods of time. The reaction mixture for the DddD assay was supplemented with 10 µM acetyl-CoA, which takes the methyl group removed from DMSP, and that for the DmdA assay was set up in anaerobic conditions with 0.685 mM tetrahydrofolate (THF), required as a cofactor. At definite time intervals, the reaction was quenched by filtering through Amicon Ultra-4 or Ultra-15 30 K (Millipore Sigma) with centrifugation at 5000 × g for 10 min and 4°C for DMSP quantification and S isotope measurements.

Table 1. List of *E. coli* BL21 clones expressing different genes involved in DMSP degrading pathways utilized in this study.

Gene	Pathway	Cloned in <i>E. coli</i> from	Reference
dmdA	Demethylation	<i>Ruegeria pomeroyi</i> DSS-3 (Roseobacter; α-Proteobacteria)	Reisch et al. (2008)
alma1	Cleavage (DMS + acrylate)	<i>Emiliania huxleyi</i> (Coccolithophore)	Alcolombri et al. (2015)
dddP	Cleavage (DMS + acrylate)	<i>Ruegeria pomeroyi</i> DSS-3 (Roseobacter; α-Proteobacteria)	Todd et al. (2011)
dddY	Cleavage (DMS + acrylate)	<i>Desulfovibrio acrylicus</i> (δ-Proteobacteria)	Lei et al. (2018b)
dddK	Cleavage (DMS + acrylate)	<i>Pelagibacter ubique</i> (SAR11; α-Proteobacteria)	Lei et al. (2018b)
dddQ	Cleavage (DMS + acrylate)	<i>Ruegeria pomeroyi</i> DSS-3 (Roseobacter; α-Proteobacteria)	Todd et al. (2011)
dddD	Cleavage (DMS + 3-HP-CoA)	<i>Marinomonas MWYL1</i> (γ-Proteobacteria)	Alcolombri et al. (2014b)

Dimethylsulfoniopropionate quantification

For DMSP separation and quantification, an Acquity™ ultra-performance liquid chromatograph (Waters, Milford, Massachusetts) coupled to a Xevo G2-S electrospray ionization quadrupole time-of-flight mass spectrometer (Waters Micro-mass, Manchester, England) operated in positive ion mode [UPLC/(+) ESI-Q-TOF-MS] was used. Samples were prepared by diluting the stopped DMSP reactions 1:100 in acetonitrile to fall into the linear detection range of 1.5–30 μM . The UPLC separation was carried out with an Acquity UPLC™ BEH HILIC column (1.7 μm , 2.1 mm \times 100 mm) kept at 27°C with water (solvent A) and acetonitrile (solvent B) following the same gradient used by Spielmeyer and Pohnert (2010). The separation started with 10% A at a flow rate of 0.25 mL/min for 0.4 min. The gradient was linearly increased to 60% A until 1.7 min. At 1.9 min, the flow rate was increased to 0.6 mL/min. At 2.7 min, the flow rate and gradient were set back to 0.25 mL/min and 10% A. Finally, the column was equilibrated for 1.3 min, resulting in a total analysis time of 4 min. Calibration was performed with standards from 1 to 30 μM DMSP, and each sample was diluted for quantification within this range. The retention time of DMSP was 2.4 min. Acetonitrile containing 5% v/v water was used as the working fluid in the autosampler syringe in order to maintain the low water content of the sample solution and initial mobile phase concentration that is critical for successful HILIC chromatography. The mass range from 50 to 300 m/z using a scan rate of 0.3 s was recorded. The injection volume was 1 μL and the sample was kept at 4°C. The optimized ESI parameters used were 3 kV capillary voltage, 40 V sampling cone, 80 V source offset, 120°C source temperature, 450°C desolvation temperature, and 6 V collision energy.

MS–MS mode data were also acquired to eliminate the possibility of isobaric interferences. For this measurement, the quadrupole was set to pass a range of ± 1 m/z around the mass of the parent ion (134 m/z). The collision energy was increased to 30 V, and the signal between 50 and 300 m/z was recorded at high resolution in the time-of-flight analyzer. The product ion at 73 m/z was used for quantitation. Instrumental stability (i.e., chromatographic and mass spectral reproducibility) was verified within 5% using a standard solution of DMSP (Sigma-Aldrich) run periodically (one standard every 10 samples) during routine analysis. Data were acquired and processed using MassLynx v4.1 software. The enzymatic rates of DMSP consumption over time were fitted to Michaelis–Menten kinetics using the previously reported Michaelis–Menten constant (K_M) for each heterologously expressed enzyme (same references as those in Table 1 except for DddP (Kirkwood et al. 2010), DddK (Peng et al. 2019), and DddQ (Burkhardt et al. 2017).

Sulfur isotope analysis

To determine the isotopic composition of the residual DMSP (leftover DMSP after the enzymatic reaction) over the

course of the enzyme assays, a volume of supernatant from the quenched reactions containing 3–5 μg of S was freeze dried, resuspended in distilled water, and allowed to evaporate in tin capsules heated at 60°C to concentrate DMSP and remove volatile sulfur. Sulfur was measured as SO_2 by EA-IRMS (Carlo Erba NC 2500 Elemental Analyzer connected to a Delta + XL, ThermoQuest, via the Thermo ConFlo III interface). We report sulfur isotope ratios using the conventional delta notation relative to the international standard Vienna-Canyon Diablo Troilite (VCDT)

$$\delta^{34}\text{S} = \left({}^{34}\text{R}_{\text{sample}} / {}^{34}\text{R}_{\text{VCDT}} \right) - 1, \quad (1)$$

where ${}^{34}\text{R}$ refers to the ${}^{34}\text{S}/{}^{32}\text{S}$ ratio. The values of each sample were corrected by subtracting the blank and using a linear interpolation between two in-house working standards (sulfanilamide and seawater), with an analytical repeatability better than 0.26‰.

The sulfur isotope fractionation factors for each enzyme (${}^{34}\epsilon_{\text{enz}}$) were calculated from the slope of the linear regression analysis of the most accurate approximate solution to the Rayleigh distillation equation (Mariotti et al. 1981; Scott et al. 2004):

$$\ln(1 + \delta^{34}\text{S}_{\text{DMSP}}) = \ln(1 + \delta^{34}\text{S}_{\text{DMSP},0}) - {}^{34}\epsilon_{\text{enz}} \cdot \ln(f_R) \quad (2)$$

where enz can be replaced by any of the enzymes studied, f_R is the fraction of remaining DMSP in the assay vials, and $\delta^{34}\text{S}_{\text{DMSP},0}$ and $\delta^{34}\text{S}_{\text{DMSP}}$ are the sulfur isotopic compositions of the initial and remaining DMSP at the time of the measurement, respectively. The details of the corrections performed are included in the Supporting Information.

Data analysis

For the analysis of the data—both the substrate degradation kinetics and the inference of the fractionation factor—we took a Bayesian analysis approach. A full description of how this analysis was performed, including both the theoretical background and the assumptions behind the statistical analysis, can be found in the Supporting Information.

Data and code availability

All data and custom scripts were collected and stored using Git version control. Code for raw data processing, analysis, modeling, and figure generation is available in the GitHub repository (<https://github.com/daniosro/DMSP>).

Results

The DMSP concentration in the reaction vials at different timepoints in the enzyme assays with DmdA (DMSP demethylase) or various DMSP lyases are shown in Fig. 1. Their fits to Michaelis–Menten reaction kinetics were good for DmdA, Alma1 and DddK, and satisfactory for DddD and DddY

(Fig. S1). However, we noticed that in the case of DddP and DddQ the curves seem to flatten out before the reactions were completed. This was not surprising, since a low catalytic activity for both enzymes has been recognized (Alcolombri et al. 2014a; Wang et al. 2015). To investigate if a deviation from Michaelis–Menten kinetics in these enzymes could be explained by a loss of their activity during the course of the reactions, we repeated the Michaelis–Menten fit incorporating a first order decay rate for the enzymes. If an enzyme loses activity over the course of the reaction, its concentration in the assay vial (E) is assumed to decrease following a first order rate (k):

$$\frac{dE}{dt} = -kE \quad (3)$$

In turn, the change in the concentration of DMSP over time will be affected by the decrease in the amount of enzyme:

$$\frac{d\text{DMSP}}{dt} = \frac{-v_{\max} E \text{DMSP}}{K_M + \text{DMSP}} \quad (4)$$

Where K_M is the previously reported Michaelis–Menten constant (see the Methods section) and v_{\max} is the fitted maximum velocity per enzyme (units of nM substrate/min), such

that V_{\max} , the maximum catalytic activity when the enzyme is saturated, is equal to $v_{\max}E$. The results of this modeling show very good agreement with the data (Fig. 1). We performed additional enzyme assays for Alma1, the enzyme with the highest activity, in order to get experimental support for this hypothesis (Supporting Information). When the enzyme is in a very low concentration, the reaction stalls early and when most of the DMSP is still remaining in the reaction. Adding higher concentrations of enzyme proportionally increases the fraction of DMSP degraded. Similarly, when additional DMSP is added to reaction vials where most of it was already consumed, the added DMSP was degraded very slowly (Fig. S2). Thus, the experimental results validate the modeled prediction of a loss of enzymatic activity over the course of the DMSP degradation assays.

Despite reacting DMSP with large concentrations of DddP and DddQ, the enzymes that seem to exhibit the larger loss of activity, we still could not detect complete degradation of DMSP by these enzymes. To establish if this could affect the fractionation factors calculated below from the isotopic compositions of DMSP over the course of the enzymatic degradation experiments, we performed modeling for DddP. We integrated Eqs. 3 and 4 for $^{34}\text{DMSP}$ and $^{32}\text{DMSP}$ (more details are provided in the Supporting Information), and used their values to compute the $\delta^{34}\text{S}$ of DMSP for $k = 0$ and $k = 0.08$. We determined the theoretic fractionation factors ($^{34}\epsilon$) from

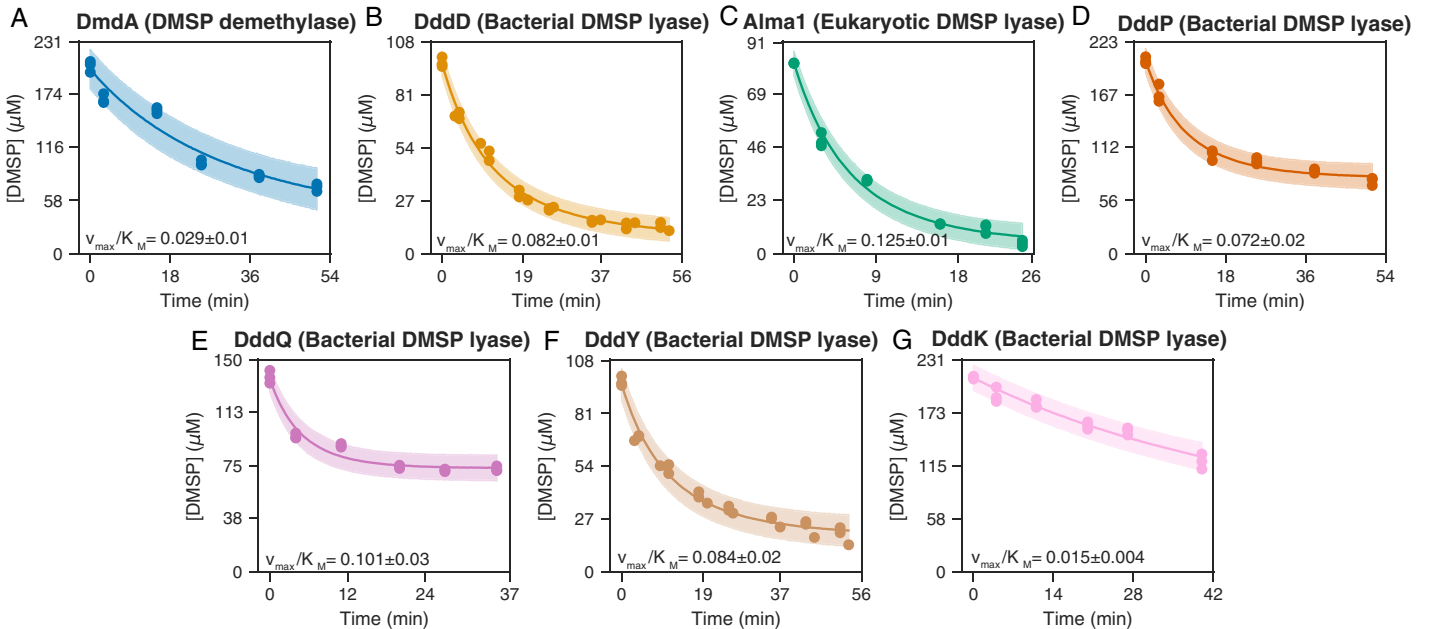


Fig 2. Degradation of DMSP by the enzymes depicted in Fig. 1: **(A)** DmdA, which catalyzes the demethylation pathway; **(B)** DddD, which catalyzes the cleavage pathway with the production of 3-HP-CoA; **(C)** Alma1, which is the only eukaryotic DMSP lyase described; **(D)** DddP, the most abundant and expressed bacterial DMSP lyase; and **(E)** DddQ, **(F)** DddY, and **(G)** DddK, other DMSP lyases. The points are combined data from triplicate measurements for each enzyme and the lines represent a fit of the reaction rate based on the Michaelis–Menten kinetics, assuming that the enzymes lose activity over time with a first order degradation rate. v_{\max}/K_M is the effective catalytic rate of each enzyme, in min^{-1} . Shaded regions represent the 95% credible intervals from the Bayesian inference of Michaelis–Menten kinetics with enzyme degradation.

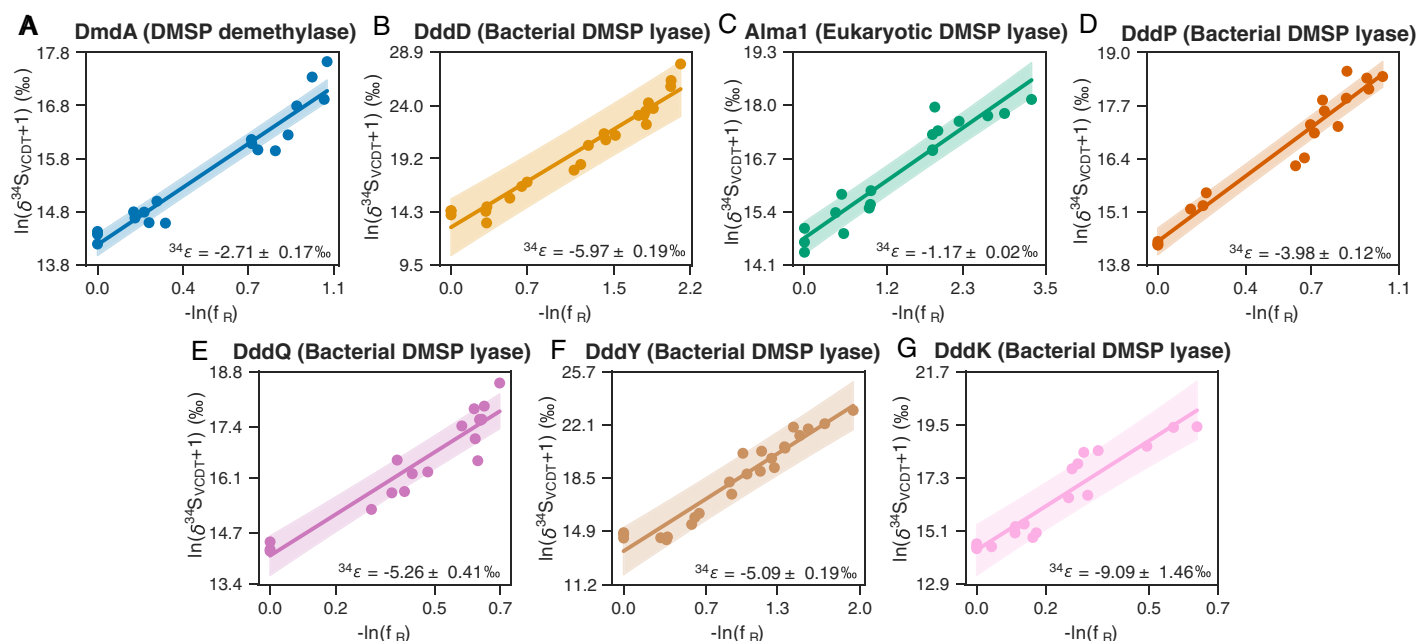


Fig 3. Evolution of the $\delta^{34}\text{S}$ values of DMSP as it is degraded by (A) DmdA, which catalyzes the demethylation pathway; (B) DddD, which catalyzes the cleavage pathway with the production of 3-HP-CoA; (C) Alma1, which is the only eukaryotic DMSP lyase described; (D) DddP, the most abundant and expressed bacterial DMSP lyase, and (E) DddQ, (F) DddY, and (G) DddK, other DMSP lyases. Measurements were made at the same points as the concentrations depicted in Fig. 1. The points are combined data from triplicate measurements for each enzyme. Values of $\ln(\delta^{34}\text{S}_{\text{DMSP}} + 1)$ are plotted against the negative \ln of the fraction of DMSP remaining (f_R). The lines represent a linear fit of the Rayleigh distillation equation, where the slope was taken as a measurement of the fractionation factor, $^{34}\epsilon$. Shaded regions represent the 95% credible intervals from the Bayesian inference of the linear regression.

the slope of the regression of $\ln(\delta^{34}\text{S}_{\text{DMSP}} + 1)$ vs. $\ln f_R$ (fraction of DMSP remaining) in both cases, as described in the Methods section. We found that the apparent loss of enzyme activity should not affect the enrichment factors by more than 0.01‰ (Fig. S3A,B). If the enzyme activity was kept constant, the $\delta^{34}\text{S}$ values of DMSP that we measured would be larger, because they would be driven to a greater extent of reaction (more DMSP degradation) than under a loss of enzyme activity. In the two cases, there would be a substantial difference in the $\ln(\delta^{34}\text{S}_{\text{DMSP}} + 1)$ as a function of time, but not as a function of $\ln f_R$ (Fig. 3C).

Since there is no way to discern if the isotope effects of the DMSP degrading enzymes impact V_{max} only, K_M only or both, the previous model had to make assumptions about them for both ^{34}S and ^{32}S , as well as about the rate of loss of enzyme activity. To guarantee the reliability of the fractionation factors that we determined, we performed sensitivity tests to determine how much the fractionation factors at steady-state would change for different enzyme degradation rates, $^{32}V_{\text{max}}$ and $^{32}V_{\text{max}}/^{32}K_M$. We found that changing $^{32}V_{\text{max}}$ (or $^{34}V_{\text{max}}$) would have a negligible impact on the fractionation factor, whereas changing $^{32}V_{\text{max}}/^{32}K_M$ (or $^{34}V_{\text{max}}/^{34}K_M$) would only change it by 0.02‰ (Fig. S4). These analyses are fully described in the Supporting Information and allowed us to further confirm that the fractionation factors determined from the $\delta^{34}\text{S}$ values of DMSP that we measured are reliable.

Having established that a loss of enzyme activity should not affect the measured $\delta^{34}\text{S}$ values, we used them together with the fractions of DMSP remaining in each enzymatic reaction at each data point to calculate the fractionation factors ($^{34}\epsilon$, Fig. 2). All of the enzymes evaluated were found to have normal kinetic isotope effects (i.e., negative fractionation factors), that range between -1.2 and -9.1 ‰.

Discussion

The fractionation factors ($^{34}\epsilon$) determined here are negative (normal isotope effects), span a range of ~ 8 ‰, and are not correlated with the effective catalytic rate (v_{max}/K_M) or the Michaelis–Menten constant (K_M) of each enzyme. These $^{34}\epsilon$ values are small compared to those of other biological sulfur transformations such as sulfate reduction (Sim et al. 2011) and sulfur disproportionation (Canfield and Thamdrup 1994). The most plausible reason is that the cleavage of the C–S bond is not the rate-limiting step in the reaction, and therefore, there is little sensitivity to sulfur isotopes once this step takes place (i.e., Goldstein 1966). Specifically, in the case of the DMSP lyases that cleave DMSP to DMS and acrylate, the sulfur cleavage reaction happens near the end of a cascade that is initiated by removing the hydrogen from the alpha carbon position (Fig. S5). The larger the reversibility of this H abstraction step, the larger the size of the kinetic isotope effect on the S

isotopes of the residual (remaining) DMSP (Kaplan and Rittenberg 1964). This expected trend matches our observations, since the magnitude of the fractionation factors ($\text{Alma1} < \text{DddP} < \text{DddY} \sim \text{DddQ} < \text{DddK}$) is correlated with the reversibility of the reactions. Alma1 uses cysteine as a nucleophile (Alcolombri et al. 2015), whereas DddP uses aspartate and coordination to a Fe atom (Wang et al. 2015), DddY and DddQ have DMSP coordinated to a Zn (sometimes Fe) atom and use tyrosine as nucleophile (Li et al. 2014), and DddK uses tyrosine as well but coordinates DMSP to a Mn or Ni atom (Schnicker et al. 2017; Peng et al. 2019, Fig. S5). Thus, the DMSP cleavage reactions with acrylate as a byproduct in which a stronger nucleophile is involved (i.e., cysteine) are less reversible than those where a weaker nucleophile is involved (i.e., tyrosine), and consequently have smaller isotope effects.

Despite the diversity of DMSP degrading enzymes, the Tara Oceans expedition found that more than 90% of the expressed bacterial DMSP lyases (fraction $<3\ \mu\text{m}$) are DddP homologs (Curson et al. 2018; Fig. S6). Thus, we modeled the expected $\delta^{34}\text{S}$ values of total DMSP in seawater assuming that DMSP is either demethylated or cleaved by only Alma1 (eukaryotic DMSP lyase) or DddP, incorporating our fractionation factors in the calculations. The model is described in detail in the Supporting Information, and the results for different activities of each enzyme are shown in Fig. 4. We considered the ocean as a single box with a constant inward flux of DMSP from a single process (biosynthesis) and two possible outward fluxes, cleavage, and demethylation. The mixing ratio between the three possible consumption pathways for DMSP that our model considers—demethylation, bacterial cleavage by DddP, and eukaryotic cleavage by Alma1—will determine the $\delta^{34}\text{S}$ of total DMSP in seawater. It would be expected that the fractionation by Alma1 would be primarily imparted in the particulate DMSP pool, and that the fractionation by bacterial enzymes would be imparted in the dissolved DMSP pool, although our model does not differentiate between these two. If the production of DMSP is balanced by consumption (a reasonable assumption in the ocean due to the rapid turnover of DMSP), mass balance constrains the isotopic composition of total DMSP to be different from the input by the isotope effect (Hayes 2001). In other words, the isotopic composition inherited by DMSP from its biosynthetic pathway is subsequently altered by consumption, and the enzyme with a higher concentration (due to differences in community composition and/or gene expression) or activity (faster reaction rates) will drive the $\delta^{34}\text{S}$ of total DMSP toward its fractionation value. As a consequence, when eukaryotic cleavage is the dominant process (Alma1; $^{34}\epsilon \sim -1\text{‰}$), total seawater DMSP will have the lowest $\delta^{34}\text{S}$, when demethylation dominates (DmdA; $^{34}\epsilon \sim -3\text{‰}$), total seawater DMSP will have an intermediate $\delta^{34}\text{S}$ value, and when bacterial cleavage dominates, total seawater DMSP will be able to reach the heaviest possible $\delta^{34}\text{S}$ values, assuming that the input of DMSP to the ocean has

an approximately constant $\delta^{34}\text{S}$ value. Since DmdA has an intermediate fractionation factor between those of Alma1 and DddP, the $\delta^{34}\text{S}$ value of DMSP of an environmental sample would not be enough to establish whether demethylation or cleavage processes are dominant, and other biological analysis tools could be handy in these cases, as further explained below.

The value of $-1.18 \pm 0.06\text{‰}$ for the $^{34}\epsilon$ of Alma1 agrees with an $^{34}\epsilon$ of -1 to -1.5‰ reported for DMSP cleavage in culturing experiments with the macroalgae *Ulva lactuca* and *Ulva linza* (Oduro et al. 2012). To our knowledge, no other absolute fractionation factors for DMSP degrading enzymes had been reported before. Our modeling approach demonstrates their usefulness to infer the DMSP degradation processes that dominate over a seawater sample with a particular $\delta^{34}\text{S}_{\text{DMSP}}$. We predict values of total seawater $\delta^{34}\text{S}$ of DMSP that range from 18.2 to 21.1‰. These values fall within the range of $\delta^{34}\text{S}$ of total DMSP measured in seawater to date during normal (nonbloom) conditions (Amrani et al. 2013; Carnat et al. 2018), spanning 17.8–20.5‰ at depths up to 140 m, and 18.9–20.3‰ in surface waters (0–5 m). The model assumed an isotopic composition of 17‰ for newly synthesized DMSP (before it is affected by any degradation process) in order to capture the entire range of nonbloom total seawater $\delta^{34}\text{S}_{\text{DMSP}}$ measurements from those two studies. This value is lower than the data of intracellular $\delta^{34}\text{S}_{\text{DMSP}}$ reported by Oduro et al. (2012) in macroalgae ($18.2 \pm 0.6\text{‰}$) and phytoplankton ($19.6 \pm 0.3\text{‰}$), and by Gutierrez-Rodriguez et al. (2017) in *Phaeocystis* and foraminifera ($\sim 20\text{‰}$), which correspond to particulate DMSP. This indicates that there must be a normal isotope effect in the synthesis of DMSP from marine sulfate (21‰), and that the intracellular particulate $\delta^{34}\text{S}_{\text{DMSP}}$ measured by Oduro et al. (2012) and Gutierrez-Rodriguez et al. (2017) might already have been affected by cleavage by Alma1, which would leave that DMSP pool enriched in ^{34}S .

On the other hand, the values measured by Amrani et al. (2013) for the $\delta^{34}\text{S}$ of DMS in seawater were found to be consistently higher relative to the $\delta^{34}\text{S}$ of total DMSP in the same samples by an average of 0.6‰ throughout the water column. The same study found a -0.5‰ fractionation factor associated to the volatilization of DMS. The fractionation factors for DMSP cleavage reported here and the fractionation factor for DMS volatilization reported by Amrani et al. (2013) alone would not be able to explain the seawater $\delta^{34}\text{S}_{\text{DMS}}$ under normal conditions. However, under nonsteady-state conditions, such as at the end of a bloom, fast recycling of organic sulfur compounds might increase the $\delta^{34}\text{S}_{\text{DMS}}$ values. The only other processes that could cause fractionation of S isotopes in DMS are consumption by organisms and photooxidation. If photooxidation was responsible for the enrichment of ^{34}S in DMS relative to DMSP, Gutierrez-Rodriguez et al. (2017) should have found $^{34}\epsilon$ values different than those reported by Oduro et al. (2012), since these studies performed incubations

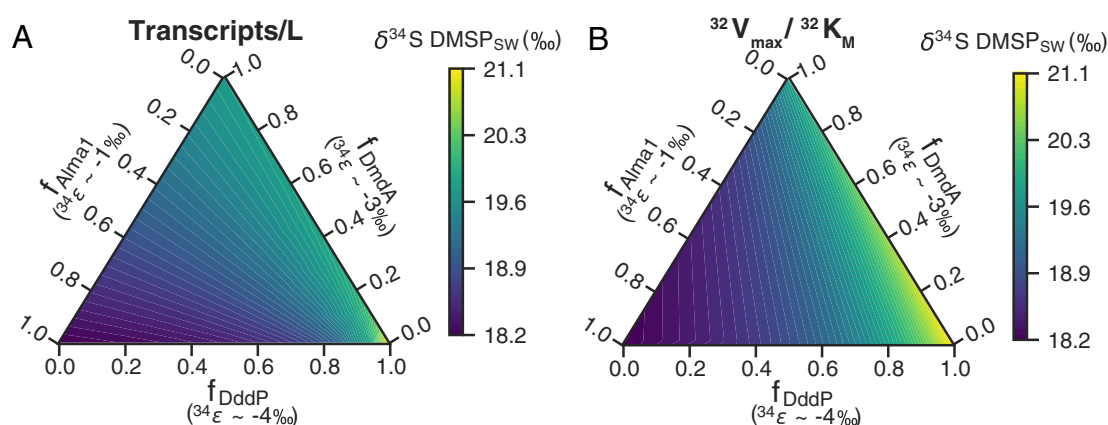


Fig 4. Prediction of the $\delta^{34}\text{S}$ values of total DMSP in seawater (SW, colorbars), assuming that DMSP is degraded only by Alma1 (eukaryotic DMSP lyase), DddP (most abundant bacterial DMSP lyase), and DmdA (DMSP demethylase). The isotopic mass balance calculation assumed a $\delta^{34}\text{S}$ of 17‰ for the incoming flux of DMSP. The ternary plots show the expected S isotopic composition of total DMSP when Alma1, DddP and DmdA fractionally contribute to DMSP degradation amounting to a total of 1 (or 100%), when that contribution is considered in terms of **(A)** the enzyme concentrations in transcripts per liter or **(B)** the enzyme catalytic rate for the light and most abundant isotope of sulfur (^{32}S , $^{32}V_{\text{max}}/^{32}K_M$) of each enzyme.

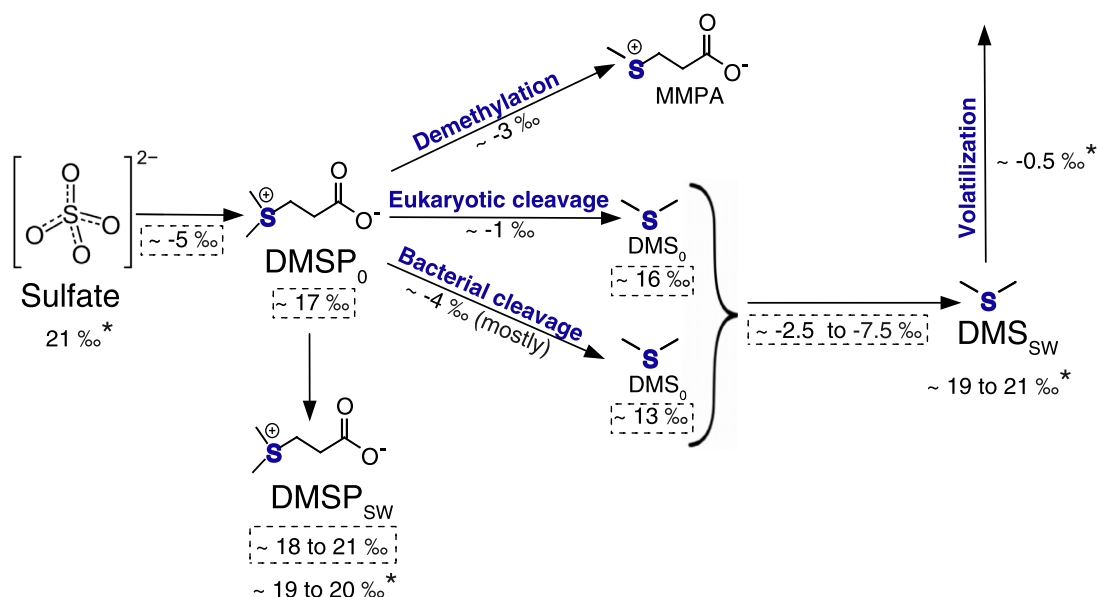


Fig 5. Schematic representation of the predicted and determined isotope fractionations associated with DMSP and DMS synthesis and degradation. The values with * were reported by Amrani et al. (2013) and the values surrounded by a dashed box are predicted based on the fractionation factors found in this study. The subscript 0 refers to just synthesized DMSP or DMS, and the subscript SW refers to the range of values of DMSP or DMS in seawater.

under light and dark conditions, respectively. Therefore, we propose that there must be a normal isotope effect of about -2.5 to -7.5 ‰ associated with microbial DMS consumption, which drives the residual DMS back to a $\delta^{34}\text{S}$ close to that of seawater sulfate (Fig. 5). This was previously hypothesized by Amrani et al. (2013) and it is consistent with the observations from Gutierrez-Rodriguez et al. (2017) in seawater incubations. Alternatively, the inputs of DMSP to the ocean might have different $\delta^{34}\text{S}$ values, which would increase the range of possible $\delta^{34}\text{S}_{\text{DMS}}$ in seawater samples.

The presence of DMSP lyases in marine bacterial genomes is variable. In particular, DddK is much more abundant in high southern latitudes (Landa et al. 2019). On the other hand, it has been established that DMSP and DMS productivity is high in coastal and marine sediments, and that bacteria are important DMSP producers in these environments (Williams et al. 2019). Some DMSP lyases that do not have a high representation in the global ocean metatranscriptomes, such as DddD and DddY (Fig. S6), have been isolated from coastal and intertidal settings (De Souza and Yoch 1995; Todd

et al. 2007; Curson et al. 2011), in association with plant roots and microaerobic environments. These differences could be responsible for local variability in the $\delta^{34}\text{S}$ of environmental DMSP. Studies based on the tracing of ^{35}S -labeled DMSP (Kiene and Linn 2000) and the quantification of sulfur species (Bates 1994) determined that usually less than 30% of DMSP is cleaved in natural waters. This would imply that demethylation is the dominant DMSP-degrading process over most of the ocean, and it is consistent with the presence of DmdA in 19% of the Tara Oceans' surveyed bacterial genomes from all depths, vs. that of all of the bacterial DMSP lyases combined in only 9% of them (Landa et al. 2019). It has also been pointed out that in global surface waters *dmdA* homologs are present in more than 50% of free living bacterioplankton, whereas genes that encode DMSP lyases are up to two orders of magnitude less abundant (Moran et al. 2012). The average value of total seawater $\delta^{34}\text{S}_{\text{DMSP}}$ from Amrani et al. (2013) (19.6‰) and those of ~19–20‰ predicted by our model are reasonable if demethylation is the dominant DMSP degradation process. It has also been established that the transcripts of DmdA are about one order of magnitude more abundant than those of DddP in the open ocean (Levine et al. 2012; Varaljay et al. 2015), and that both increase during algal blooms (Varaljay et al. 2015). Transcriptomic data for Alma1, the eukaryotic DMSP lyase (Vorobev et al. 2020, Fig. S6), also indicate higher expression levels of this enzyme in the Southern Ocean and the North Atlantic Ocean, where high DMSP producers like *Phaeocystis* and coccolithophores thrive (Yoch 2002). However, no Alma1 transcripts were found in most of the stations sampled by the Tara Oceans expedition in these and other ocean basins (Fig. S6). This suggests that the expression of Alma1 is mostly limited to localized spots in the ocean, possibly associated with eukaryotic blooms. If that was the case, and its expression dominated over that of bacterial DMSP lyases during those blooms, the particulate (and total) $\delta^{34}\text{S}_{\text{DMSP}}$ would be driven closer to that of the source, because of its small normal isotope effect and the shift in community composition. Slightly higher values of total $\delta^{34}\text{S}_{\text{DMSP}}$ were measured by Amrani et al. (2013) in a Greenland bloom in samples kept at 25°C (19.5–22.1‰) relative to nonbloom conditions. This bloom was dominated by the high DMS/P producer *Emiliania huxleyi*, and the wide range of total $\delta^{34}\text{S}_{\text{DMSP}}$, both above and below the $\delta^{34}\text{S}$ of seawater, might reflect a rapid recycling of organic sulfur during blooms dominated by high DMS/P producing algae. In the same study, the values of total $\delta^{34}\text{S}_{\text{DMSP}}$ of a Mediterranean Sea bloom, dominated by small eukaryotes and the cyanobacteria *Synechococcus*, were not different from those of nonbloom conditions, which is consistent with an interplay between bacterial and eukaryotic DMSP degradation processes when blooms retain a mixed community composition. More studies on ecosystem and community composition changes during blooms and across different oceanic regimes are required to address these differences.

Conclusions

The fractionation factors reported here provide an indication of the biological fates of DMSP in the ocean. For most of the ocean, the total $\delta^{34}\text{S}_{\text{DMSP}}$ values result from a mixed contribution from demethylation, bacterial cleavage and eukaryotic cleavage. Our data can be useful to address whether bacterial or eukaryotic DMSP degrading processes dominate at a local scale. Since the bacterial DMSP lyases have higher fractionation factors (approx. –4 to –9‰), samples with heavier-than-average $\delta^{34}\text{S}_{\text{DMSP}}$ measurements might provide key clues to address why the switch from demethylation to cleavage happens in bacteria (Simó 2001). More measurements of dissolved and total seawater $\delta^{34}\text{S}_{\text{DMSP}}$, tied to microbial metagenomics and metatranscriptomics, are needed to fully understand how seawater $\delta^{34}\text{S}_{\text{DMSP}}$ values are affected by ecological dynamics, and could also be critical to understanding the role and evolution of the DMSP degrading enzymes. Additionally, identifying the S isotope fractionations imparted by DMSP biosynthesis and biological DMS consumption will be critical to improve our understanding of relative importance of bacteria and algae in the cycling of organic S and the implications of these processes for marine microbial communities.

References

- Alcolombri, U., S. Ben-Dor, E. Feldmesser, Y. Levin, D. S. Tawfik, and A. Vardi. 2015. Identification of the algal dimethyl sulfide-releasing enzyme: A missing link in the marine sulfur cycle. *Science* **348**: 1466–1469.
- Alcolombri, U., M. Elias, A. Vardi, and D. S. Tawfik. 2014a. Ambiguous evidence for assigning DddQ as a dimethylsulfoniopropionate lyase and oceanic dimethylsulfide producer. *Proc. Natl. Acad. Sci.* **111**: 2078–2079. doi:10.1073/pnas.1401685111
- Alcolombri, U., P. Laurino, P. Lara-Astiaso, A. Vardi, and D. S. Tawfik. 2014b. DddD is a CoA-transferase/lyase producing dimethyl sulfide in the marine environment. *Biochemistry* **53**: 5473–5475. doi:10.1021/bi500853s
- Amrani, A., W. Said-Ahmad, Y. Shaked, and R. P. Kiene. 2013. Sulfur isotope homogeneity of oceanic DMSP and DMS. *Proc. Natl. Acad. Sci.* **110**: 18413–18418.
- Barak-Gavish, N., M. J. Frada, C. Ku, and others. 2018. Bacterial virulence against an oceanic bloom-forming phytoplankton is mediated by algal DMSP. *Sci. Adv.* **4**: eaau5716. doi:10.1126/sciadv.aau5716
- Bates, T. S. 1994. The cycling of sulfur in surface seawater of the Northeast Pacific. *J. Geophys. Res.* **99**: 7835–7843. doi:10.1029/93JC02782
- Burkhardt, I., L. Lauterbach, N. L. Brock, and J. S. Dickschat. 2017. Chemical differentiation of three DMSP lyases from the marine: Roseobacter group. *Org. Biomol. Chem.* **15**: 4432–4439. doi:10.1039/c7ob00913e

- Canfield, D. E., and B. Thamdrup. 1994. The production of ^{34}S -depleted sulfide during bacterial disproportionation of elemental sulfur. *Science* **266**: 1973–1975. doi:[10.1126/science.11540246](https://doi.org/10.1126/science.11540246)
- Carnat, G., W. Said-ahmad, F. Fripiat, B. Wittek, J. Tison, C. Uhlig, and A. Amrani. 2018. Variability in sulfur isotope composition suggests unique dimethylsulfoniopropionate cycling and microalgae metabolism in Antarctic Sea ice. *Commun. Biol.* **1**: 212. doi:[10.1038/s42003-018-0228-y](https://doi.org/10.1038/s42003-018-0228-y)
- Charlson, R. J., J. E. Lovelock, M. O. Andreae, and S. G. Warren. 1987. Ocean phytoplankton, atmospheric sulfur, cloud albedo, and climate. *Nature* **326**: 655–661.
- Curson, A. R. J., M. J. Sullivan, J. D. Todd, and A. W. B. Johnston. 2011. DddY, a periplasmic dimethylsulfoniopropionate lyase found in taxonomically diverse species of Proteobacteria. *ISME J.* **5**: 1191–1200. doi:[10.1038/ismej.2010.203](https://doi.org/10.1038/ismej.2010.203)
- Curson, A. R. J., B. T. Williams, B. J. Pinchbeck, and others. 2018. DSYB catalyses the key step of dimethylsulfoniopropionate biosynthesis in many phytoplankton. *Nat. Microbiol.* **3**: 430–439. doi:[10.1038/s41564-018-0119-5](https://doi.org/10.1038/s41564-018-0119-5)
- Dickson, D. M. J., and G. O. Kirst. 1987. Osmotic adjustment in marine eukaryotic algae: The role of inorganic ions, quaternary ammonium, tertiary sulphonium and carbohydrate solutes: I. Diatoms and a rhodophyte. *New Phytol.* **106**: 645–655.
- Fakhraee, M., and S. Katsev. 2019. Organic sulfur was integral to the Archean sulfur. *Nat. Commun.* **10**: 1–8. doi:[10.1038/s41467-019-12396-y](https://doi.org/10.1038/s41467-019-12396-y)
- Fike, D. A., A. S. Bradley, and C. V. Rose. 2015. Rethinking the ancient sulfur cycle. *Annu. Rev. Earth Planet. Sci.* **43**: 593–622.
- Galí, M., and R. Simó. 2015. A meta-analysis of oceanic DMS and DMSP cycling processes: Disentangling the summer paradox. *Global Biogeochem. Cycles* **29**: 496–515. doi:[10.1002/2014GB004940](https://doi.org/10.1002/2014GB004940)
- Garrels, R. M., and A. Lerman. 1981. Phanerozoic cycles of sedimentary carbon and sulfur. *Proc. Natl. Acad. Sci.* **78**: 4652–4656. doi:[10.1073/pnas.78.8.4652](https://doi.org/10.1073/pnas.78.8.4652)
- Goldstein, M. J. 1966. Kinetic isotope effects and organic reaction mechanisms. *Nature* **154**: 1616–1621.
- Gutierrez-Rodriguez, A., L. Pillet, T. Biard, W. Said-Ahmad, A. Amrani, R. Simó, and F. Not. 2017. Dimethylated sulfur compounds in symbiotic protists: A potentially significant source for marine DMS(P). *Limnol. Oceanogr.* **62**: 1139–1154. doi:[10.1002/lno.10491](https://doi.org/10.1002/lno.10491)
- Hayes, J. M. 2001. Fractionation of carbon and hydrogen isotopes in biosynthetic processes. *Rev. Mineral. Geochemistry* **43**: 225–277.
- Holland, H. D. 1973. Systematics of the isotopic composition of sulfur in the oceans during the Phanerozoic and its implications for atmospheric oxygen. *Geochim. Cosmochim. Acta* **37**: 2605–2616.
- Johnson, W. M., M. C. Kido Soule, and E. B. Kujawinski. 2016. Evidence for quorum sensing and differential metabolite production by a marine bacterium in response to DMSP. *ISME J.* **10**: 2304–2316. doi:[10.1038/ismej.2016.6](https://doi.org/10.1038/ismej.2016.6)
- Jorgensen, B. B. 1982. Mineralization of organic matter in the sea bed—the role of sulphate reduction. *Nature* **296**: 643–645.
- Kaplan, I. R., and S. C. Rittenberg. 1964. Microbiological fractionation of sulphur isotopes. *J. Gen. Microbiol.* **34**: 195–212. doi:[10.1099/00221287-34-2-195](https://doi.org/10.1099/00221287-34-2-195)
- Karsten, U., K. Kück, C. Vogt, and G. O. Kirst. 1996. Dimethylsulfoniopropionate production in phototrophic organisms and its physiological functions as a cryoprotectant, p. 143–153. *In* R. P. Kiene, P. T. Visscher, M. D. Keller, and G. O. Kirst [eds.], *Biological and environmental chemistry of DMSP and related Sulfonium compounds*. Springer.
- Keller, M. D. 1989. Dimethyl sulfide production and marine phytoplankton: The importance of species composition and cell size. *Biol. Oceanogr.* **6**: 375–382. doi:[10.1080/01965581.1988.10749540](https://doi.org/10.1080/01965581.1988.10749540)
- Kiene, R. P., and L. J. Linn. 2000. The fate of dissolved dimethylsulfoniopropionate (DMSP) in seawater: Tracer studies using ^{35}S -DMSP. *Geochim. Cosmochim. Acta* **64**: 2797–2810.
- Kiene, R. P., and D. Slezak. 2006. Low dissolved DMSP concentrations in seawater revealed by small-volume gravity filtration and dialysis sampling. *Limnol. Oceanogr. Methods* **4**: 80–95.
- Kirkwood, M., N. E. Le Brun, J. D. Todd, and A. W. B. Johnston. 2010. The dddP gene of *Roseovarius nubinhibens* encodes a novel lyase that cleaves dimethylsulfoniopropionate into acrylate plus dimethyl sulfide. *Microbiology* **156**: 1900–1906. doi:[10.1099/mic.0.038927-0](https://doi.org/10.1099/mic.0.038927-0)
- Kirst, G. O., C. Thiel, H. Wolff, J. Nothnagel, M. Wanzek, and R. Ulmke. 1991. Dimethylsulfoniopropionate (DMSP) in icealgae and its possible biological role. *Mar. Chem.* **35**: 381–388.
- Ksionzek, K. B., O. J. Lechtenfeld, S. L. McCallister, P. Schmitt-Kopplin, J. K. Geuer, W. Geibert, and B. P. Koch. 2016. Dissolved organic sulfur in the ocean: Biogeochemistry of a petagram inventory. *Science* (80–) **354**: 456–459.
- Landa, M., A. S. Burns, B. P. Durham, and others. 2019. Sulfur metabolites that facilitate oceanic phytoplankton—Bacteria carbon flux. *ISME J.* **13**: 2536–2550. doi:[10.1038/s41396-019-0455-3](https://doi.org/10.1038/s41396-019-0455-3)
- Lei, L., U. Alcolombri, and D. S. Tawfik. 2018a. Biochemical profiling of DMSP Lyases, p. 269–289. *In* *Methods in enzymology*. Elsevier.
- Lei, L., K. P. Cherukuri, U. Alcolombri, D. Meltzer, and D. S. Tawfik. 2018b. The dimethylsulfoniopropionate (DMSP) lyase and lyase-like cupin family consists of bona fide DMSP lyases as well as other enzymes with unknown function. *Biochemistry* **57**: 3364–3377.
- Levine, N. M. 2016. Putting the spotlight on organic sulfur. *Science* (80–) **354**: 418–419. doi:[10.1126/science.aai8650](https://doi.org/10.1126/science.aai8650)
- Levine, N. M., D. A. Toole, A. Neeley, N. R. Bates, S. C. Doney, and J. W. H. Dacey. 2016. Revising upper-ocean sulfur dynamics near Bermuda: New lessons from 3 years of

- concentration and rate measurements. *Environ. Chem.* **13**: 302–313.
- Levine, N. M., V. A. Varaljay, D. A. Toole, J. W. H. Dacey, S. C. Doney, and M. A. Moran. 2012. Environmental, biochemical and genetic drivers of DMSP degradation and DMS production in the Sargasso Sea. *Environ. Microbiol.* **14**: 1210–1223.
- Li, C., T. Wei, S. Zhang, X. Chen, X. Gao, P. Wang, and B. Xie. 2014. Molecular insight into bacterial cleavage of oceanic dimethylsulfoniopropionate into dimethyl sulfide. *Proc. Natl. Acad. Sci.* **111**: 1026–1031. doi:[10.1073/pnas.1312354111](https://doi.org/10.1073/pnas.1312354111)
- Li, C., D. Zhang, X. Chen, P. Wang, W. Shi, P. Li, X. Zhang, Q. Qin, J. D. Todd, and Y. Zhang. 2017. Mechanistic Insights into Dimethylsulfoniopropionate Lyase DddY, a New Member of the Cupin Superfamily. *J. Mol. Biol.* **429**: 3850–3862. doi:[10.1016/j.jmb.2017.10.022](https://doi.org/10.1016/j.jmb.2017.10.022)
- Mariotti, A., J. C. Germon, P. Hubert, P. Kaiser, R. Letolle, A. Tardieux, and P. Tardieux. 1981. Experimental determination of nitrogen kinetic isotope fractionation: Some principles; illustration for the denitrification and nitrification processes. *Plant and Soil* **62**: 413–430. doi:[10.1007/BF02374138](https://doi.org/10.1007/BF02374138)
- Mcparland, E. L., and N. M. Levine. 2019. The role of differential DMSP production and community composition in predicting variability of global surface DMSP concentrations. *Limnol. Oceanogr.* **64**: 757–773. doi:[10.1002/lno.11076](https://doi.org/10.1002/lno.11076)
- Moran, M. A., C. R. Reisch, R. P. Kiene, and W. B. Whitman. 2012. Genomic insights into bacterial DMSP transformations. *Ann. Rev. Mar. Sci.* **4**: 523–542. doi:[10.1146/annurev-marine-120710-100827](https://doi.org/10.1146/annurev-marine-120710-100827)
- Morris, A. W., and J. P. Riley. 1966. The bromide/chlorinity and sulphate/chlorinity ratio in sea water. *Deep Sea Res.* **13**: 699–705.
- Oduro, H., K. L. Van Alstyne, and J. Farquhar. 2012. Sulfur isotope variability of oceanic DMSP generation and its contributions to marine biogenic sulfur emissions. *Proc. Natl. Acad. Sci.* **109**: 9012–9016.
- Peng, M., X. Chen, D. Zhang, X. Wang, N. Wang, P. Wang, and J. D. Todd. 2019. Structure-function analysis indicates that an active-site water molecule participates in Dimethylsulfoniopropionate cleavage by DddK. *Appl. Environ. Microbiol.* **85**: 1–11.
- Pesant, S., F. Not, M. Picheral, and S. Kandels-lewis. 2015. Open science resources for the discovery and analysis of Tara oceans data. *Sci. Data* **2**: 1–16. doi:[10.1038/sdata.2015.23](https://doi.org/10.1038/sdata.2015.23)
- Quinn, P. K., and T. S. Bates. 2011. The case against climate regulation via oceanic phytoplankton sulphur emissions. *Nature* **480**: 51–56. doi:[10.1038/nature10580](https://doi.org/10.1038/nature10580)
- Reisch, C. R., M. A. Moran, and W. B. Whitman. 2008. Dimethylsulfoniopropionate-dependent demethylase (DmdA) from *Pelagibacter ubique* and *Silicibacter pomeroyi*. *J. Bacteriol.* **190**: 8018–8024.
- Rusch, D. B., A. L. Halpern, G. Sutton, and others. 2007. The sorcerer II Global Ocean sampling expedition: Northwest Atlantic through eastern tropical Pacific. *PLoS Biol.* **5**: e77.
- Sanchez, K. J., C. L. Chen, L. M. Russell, and others. 2018. Substantial seasonal contribution of observed biogenic sulfate particles to cloud condensation nuclei. *Sci. Rep.* **8**: 1–14. doi:[10.1038/s41598-018-21590-9](https://doi.org/10.1038/s41598-018-21590-9)
- Schnicker, N. J., S. M. De Silva, J. D. Todd, and M. Dey. 2017. Structural and biochemical insights into dimethylsulfoniopropionate cleavage by cofactor-bound DddK from the Prochlorococcus marine bacterium *Pelagibacter*. doi:[10.1021/acs.biochem.7b00099](https://doi.org/10.1021/acs.biochem.7b00099)
- Scott, K. M., X. Lu, C. M. Cavanaugh, and J. S. Liu. 2004. Optimal methods for estimating kinetic isotope effects from different forms of the Rayleigh distillation equation. *Geochim. Cosmochim. Acta* **68**: 433–442. doi:[10.1016/S0016-7037\(03\)00459-9](https://doi.org/10.1016/S0016-7037(03)00459-9)
- Seymour, J. R., R. Simó, T. Ahmed, and R. Stocker. 2010. Chemoattraction to dimethylsulfoniopropionate throughout the marine microbial food web. *Science* (80-.) **329**: 342–345.
- Sim, M. S., T. Bosak, and S. Ono. 2011. Large sulfur isotope fractionation does not require disproportionation. *Science* (80-.) **333**: 74–77. doi:[10.1126/science.1205103](https://doi.org/10.1126/science.1205103)
- Simó, R. 2001. Production of atmospheric sulfur by oceanic plankton: Biogeochemical, ecological and evolutionary links. *Trends Ecol. Evol.* **16**: 287–294. doi:[10.1016/S0169-5347\(01\)02152-8](https://doi.org/10.1016/S0169-5347(01)02152-8)
- So, L. H., A. Ghosh, C. Zong, L. A. Sepúlveda, R. Segev, and I. Golding. 2011. General properties of transcriptional time series in *Escherichia coli*. *Nat. Genet.* **43**: 554–560. doi:[10.1038/ng.821](https://doi.org/10.1038/ng.821)
- Sousa, S. F., N. M. F. S. A. Cerqueira, N. F. Brás, P. A. Fernandes, and M. J. Ramos. 2014. Enzymatic “tricks”: Carboxylate shift and sulfur shift. *Int. J. Quantum Chem.* **114**: 1253–1256. doi:[10.1002/qua.24689](https://doi.org/10.1002/qua.24689)
- Spielmeyer, A. and G. Pohnert. 2010. “Direct quantification of dimethylsulfoniopropionate (DMSP) with hydrophilic interaction liquid chromatography/mass spectrometry”. *Journal of Chromatography B: Analytical Technologies in the Biomedical and Life Sciences* **878**: 3238–3242.
- De Souza, M. P., and D. C. Yoch. 1995. Comparative physiology of dimethyl sulfide production by dimethylsulfoniopropionate lyase in *Pseudomonas douderoffii* and *Alcaligenes* sp. strain M3A. *Appl. Environ. Microbiol.* **61**: 3986–3991. doi:[10.1128/aem.61.11.3986-3991.1995](https://doi.org/10.1128/aem.61.11.3986-3991.1995)
- Sunda, W., D. J. Kieber, R. P. Kiene, and S. Huntsman. 2002. An antioxidant function for DMSP and DMS in marine algae. *Nature* **418**: 317–320. doi:[10.1038/nature00851](https://doi.org/10.1038/nature00851)
- Tang, K. 2020. Chemical diversity and biochemical transformation of biogenic organic sulfur in the ocean. *Front. Mar. Sci.* **7**: 1–15. doi:[10.3389/fmars.2020.00068](https://doi.org/10.3389/fmars.2020.00068)
- Todd, J. D., A. R. J. Curson, M. Kirkwood, M. J. Sullivan, R. T. Green, and A. W. B. Johnston. 2011. DddQ, a novel,

- cupin-containing, dimethylsulfoniopropionate lyase in marine roseobacters and in uncultured marine bacteria. *Environ. Microbiol.* **13**: 427–438. doi:[10.1111/j.1462-2920.2010.02348.x](https://doi.org/10.1111/j.1462-2920.2010.02348.x)
- Todd, J. D., R. Rogers, Y. Guo Li, and others. 2007. Structural and regulatory genes required to make the gas dimethyl sulfide in bacteria. *Science* (80–). **315**: 666–669.
- Tripp, H. J., J. B. Kitner, M. S. Schwalbach, J. W. H. Dacey, L. J. Wilhelm, and S. J. Giovannoni. 2008. SAR11 marine bacteria require exogenous reduced sulphur for growth. *Nature* **452**: 741–744. doi:[10.1038/nature06776](https://doi.org/10.1038/nature06776)
- Varaljay, V. A., and others. 2015. Single-taxon field measurements of bacterial gene regulation controlling DMSP fate. *ISME J.* **9**: 1677–1686. doi:[10.1038/ismej.2015.23](https://doi.org/10.1038/ismej.2015.23)
- Vorobev, A., M. Dupouy, Q. Carradec, T. Delmont, A. Annamale, P. Wincker, and E. Pelletier. 2020. Transcriptome reconstruction and functional analysis of eukaryotic marine plankton communities via high-throughput metagenomics and metatranscriptomics. *Genome Res.* **30**: 647–659. doi:[10.1101/gr.253070.119](https://doi.org/10.1101/gr.253070.119)
- Wang, P., and others. 2015. Structural and molecular basis for the novel catalytic mechanism and evolution of DddP, an abundant peptidase-like bacterial dimethylsulfoniopropionate lyase: A new enzyme from an old fold. *Mol. Microbiol.* **98**: 289–301. doi:[10.1111/mmi.13119](https://doi.org/10.1111/mmi.13119)
- Wang, S., M. E. Maltrud, S. M. Burrows, S. M. Elliott, and P. Cameron-Smith. 2018. Impacts of shifts in phytoplankton community on clouds and climate via the sulfur cycle. *Global Biogeochem. Cycles* **32**: 1005–1026. doi:[10.1029/2017GB005862](https://doi.org/10.1029/2017GB005862)
- Williams, B. T., K. Cowles, A. Bermejo Martínez, and others. 2019. Bacteria are important dimethylsulfoniopropionate producers in coastal sediments. *Nat. Microbiol.* **4**: 1815–1825. doi:[10.1038/s41564-019-0527-1](https://doi.org/10.1038/s41564-019-0527-1)
- Wolfe, G. V., M. Steinke, and G. O. Kirst. 1997. Grazing-activated chemical defence in a unicellular marine alga. *Nature* **387**: 894–897. doi:[10.1038/43168](https://doi.org/10.1038/43168)
- Yoch, D. C. 2002. Dimethylsulfoniopropionate: Its sources, role in the marine food web, and biological degradation to Dimethylsulfid. *Appl. Environ. Microbiol.* **68**: 5804–5815. doi:[10.1128/AEM.68.12.5804](https://doi.org/10.1128/AEM.68.12.5804)
- Zubkov, M. V., B. M. Fuchs, S. D. Archer, R. P. Kiene, R. Amann, and P. H. Burkill. 2002. Rapid turnover of dissolved DMS and DMSP by defined bacterioplankton communities in the stratified euphotic zone of the North Sea. *Deep. Res. II Top. Stud. Oceanogr.* **49**: 3017–3038. doi:[10.1016/S0967-0645\(02\)00069-3](https://doi.org/10.1016/S0967-0645(02)00069-3)

Acknowledgments

We thank Dan Tawfik and Lei Lei (Weizmann Institute of Science), and William Whitman and Joe Wirth (University of Georgia, Athens), who kindly provided us the recombinant *E. coli* strains with DMSP lyases and DmdA, respectively. Guillem Salazar helped with the arrangement of the transcriptomic data. We also thank Reto Wijker, Elliot Mueller, and Thomas Hanson for useful discussions, as well as John Crounse, Fenfang Wu, and Alex Phillips for both input and technical assistance. UPLC/Q-TOF-MS was performed in the Caltech Environmental Analysis Center, which is supported by the Caltech Environmental Science and Engineering program and the Beckman Institute at Caltech. This work was supported by the Caltech Center for Environmental Microbial Interactions (CEMI) Training Grant to DOR and the National Science Foundation Grant 53994-ND2 to all authors.

Conflict of Interest

None declared.

Submitted 27 November 2020

Revised 22 March 2021

Accepted 05 July 2021

Associate editor: Lauren Juranek